Zhou *et al. Herit Sci* (2021) 9:48
https://doi.org/10.1186/s40494-021-00523-2

Heritage Science

RESEARCH ARTICLE Open Access

Characterizing the sealing materials of the merchant ship Nanhai I of the Southern Song Dynasty

Yihang Zhou[1], Kai Wang[1*], Jian Sun[2], Yong Cui[3] and Dongbo Hu[1]

Abstract

Nanhai I is a highly valuable shipwreck of the Southern Song Dynasty for studying various topics, including the shipbuilding techniques. The sealing materials are of significant importance to ensure the ship's reliability during the voyage across the ocean and they were rarely analyzed. Therefore, the sealing materials of this ship were analyzed by several analytical approaches. The sealing materials included two types, i.e., gap filler with jute fibers and surface coating without any oakum. The main components of both types of putty are calcite with minor Tung oil. The weight ratio of $Ca(OH)_2$/Tung oil range from 4.3:1 to 7.9:1 for surface coating samples and the weight ratio of $Ca(OH)_2$/organics is 3.1:1 for the gap filler sample. Additionally, we first find that the surface coating has a layered structure, where outer layers contain more Tung oil than inner layers. The innermost layer of the surface coating sample might be altered by organic acids from wood deterioration, causing its loose structure and grey color. The composite layers with different formula might be a result of balancing the costs and performances of the putty.

Keywords: Nanhai I shipwreck, Ancient putty, Sealing material, Tung oil

Introduction

Nanhai I is a merchant ship of the Southern Song Dynasty (1127–1279 AD), carrying tons of major cargos of porcelain and iron wares along with ancient currencies, jewels, glasses, seeds, etc. It was first discovered in August 1987, salvaged in whole and transferred to Guangdong Maritime Silk Road Museum in 2007. The excavation of Nanhai I officially launched in 2013 [1] and has lasted for nearly a decade till recently. Radiocarbon dating of the excavated plant samples is 1052–1270 AD and that of human bones is 983–1160 AD [1]. The chronologically latest bronze coins are "淳熙元宝" (Chun Xi Yuan Bao) of the Southern Song Dynasty, equivalent to 1174–1189 AD [2, 3]. So far, this ship is probably the best representative of the regional trading of southeast Asia during that time. One of the promotors for those prosperous maritime trades must be the advances in shipbuilding, which helped construct firm and endurable ocean-going vessels. Separated cabins were one of those advanced techniques applied on this ship. Thus, water leakage of a single cabin would not be devastating, which greatly increased the reliability of the ship. Furthermore, this technique must be incorporated with another technique to ensure bulkhead was watertight. As the ship was assembled by wood planks of hulls and bulkheads with iron nails, there have to be sealing materials filling gaps, merging seams and covering defects to guarantee the whole ship was watertight.

Such sealing materials must also have enough binding strength with wood and stability apart from waterproofing property. Lime mortar is a common inorganic material used in ancient building construction worldwide due to its excellent binding and solidification properties [4–7]. It can be modified for various purposes and performances by different additives such as fiber [8], blood [9], sticky rice [10, 11], crushed brick [12], opal [13], etc. But

*Correspondence: wangkai2004@pku.edu.cn
[1] School of Archaeology and Museology, Peking University, Beijing, China
Full list of author information is available at the end of the article

none of these modifications helps to meet the requirements of ship use, i.e., waterproofing. In the meanwhile, hydrophobic organic coating materials such as drying oils or shellac do not have enough stability in harsh ocean environment and are susceptible to biological damages. Therefore, after possibly many trials, the ancient Chinese people found lime mortar and Tung oil were compatible with each other and the mixture of them, namely Chu-nam putty, was an excellent sealing material for ship during that time. A study on the sealing material of "Huaguang No.1" ancient ship of the Southern Song Dynasty revealed the composition of it was calcite, calcium carboxylate, fatty acid esters and jute fibers [14]. Ancient putty samples from Baochuanchang Shipyard of the Ming Dynasty were composed of calcite and Tung oil as well, confirmed by pyrolysis-gas chromatography/mass spectrometry (Py-GC–MS) [15]. The quantitative analysis result by thermogravimetry (TG) and atomic absorption spectroscopy (AAS) showed the ratio of $Ca(OH)_2$ (in initial material) and tung oil was 1.4:1. However, oakum or fiber was absent in those samples from Baochuanchang Shipyard [16].

In this paper, we intend to investigate the putty samples both with and without oakum from Nanhai I shipwreck, which represent at least two different types, i.e., gap filler and surface coating. Through analysis by Fourier transform infrared spectroscopy (FTIR), X-ray diffraction (XRD), scanning electron microscope with energy dispersive spectroscopy (SEM–EDS), Py-GC–MS and thermal analysis, the compositions of the sealing material of Nanhai I ship are revealed.

Materials and methods

Samples

The sealing material samples from Nanhai I shipwreck were collected on site with the help of the excavation team. Typical examples of the sealing material are shown in Fig. 1a, shot at the right half of the stern. The bulkhead surface was covered with mottled black and white putty and the oblique gap was filled with thicker whitish putty. Typical

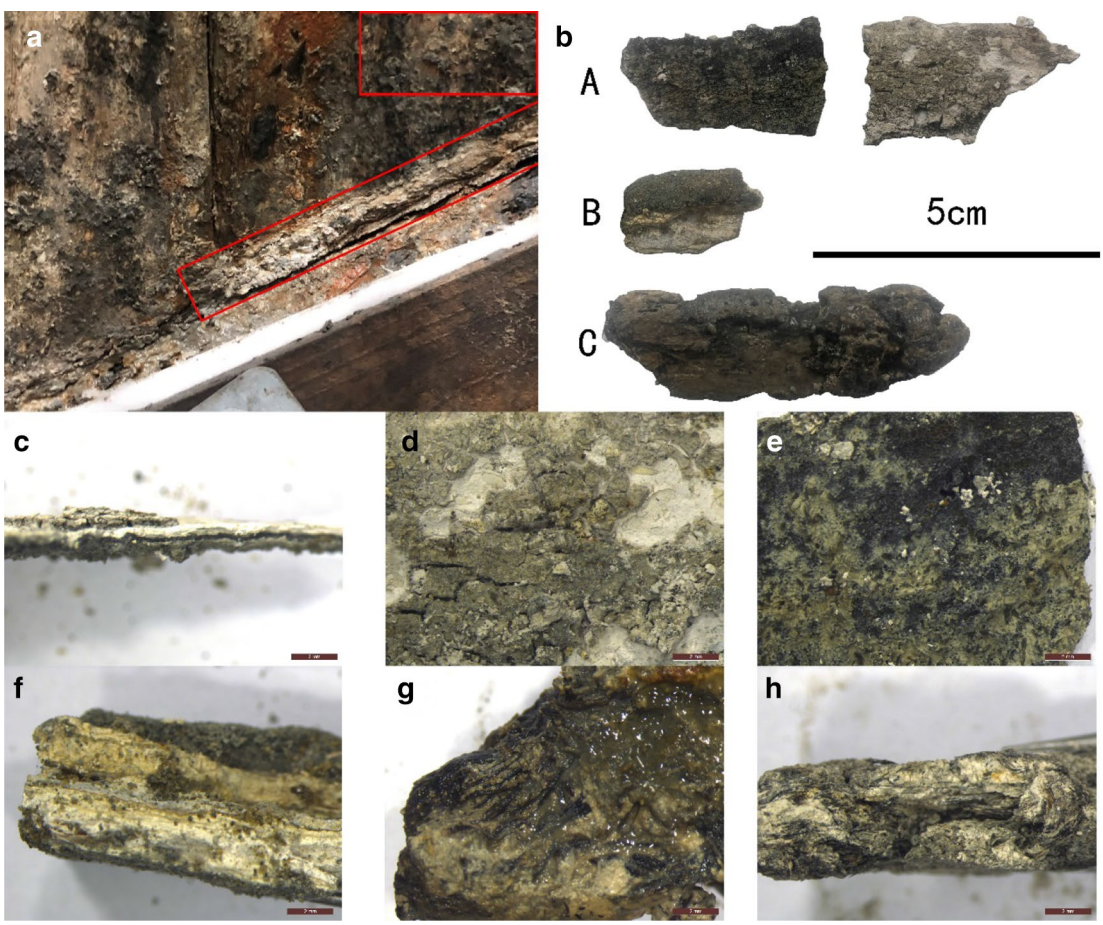

Fig. 1 The appearance of the samples: **a** sealing materials on the right stern, **b** samples A, B and C collected for analysis, **c** layered structure of sample A, **d** the inner layer of sample A, **e** the outer layer of sample A, **f** the layered structure of sample B, **g** fibers within sample C, **h** dried sample C

and better-preserved samples were selected for analysis. Sample A was collected from the surface of left larboard of C03a (the 3rd cabin), representing thin layer putty and probably for coating purpose. Sample A shown in Fig. 1b was split into two pieces, the left one showing the black outer surface and the other showing white middle layer and grey inner layer. Additional details of sample A are shown in Fig. 1c, d, e. Sample B was collected from the left stern, showing a double-layered structure (Fig. 1f). Both layers of sample B were thicker than sample A, and without black layer on the surface. The blackish material on sample B was soil sediment instead of uniform firm thin layer like sample A. Sample C was collected from the gap of the right stern, representing gap fillers with abundant fibers (wet state in Fig. 1g and dry collapsed state in Fig. 1h).

Sample preparation

Most of the samples were directly analyzed by the following approaches at the spots of interest if no preparation procedures were pointed out. Because the amount sample C is larger and it contains more organics which was speculated to be drying oil, the organics within it was extracted by ethyl acetate after acidification by 5% HCl at 50 °C for 1 h to remove calcite and convert carboxylate to carboxylic acid. The resulting organic phase was evaporated at 50 °C, yielding a brown film. The cross section of the fibers in sample C was first embedded in poly-*n*-butyl methacrylate by soaking in neat *n*-butyl methacrylate with 0.5% AIBN (azodiisobutyronitrile) at 70 °C overnight. Then the embedded fibers were cut into 15 μm thick slice by microtome, which was then observed and photoed by Leica DM4500P.

Fourier transform infrared spectroscopy (FTIR)

Samples were directly analyzed by attenuated total reflection Fourier transform infrared spectroscopy (PerkinElmer Spectrum Spotlight 200) with a range from 4000 cm^{-1} to 650 cm^{-1} under 4 cm^{-1} resolution and 128 accumulation times.

X-ray diffraction (XRD)

XRD analysis was performed on X-pert3 Powder, PANalytical with Cu anode to detect the crystals in the grinded sample. The working voltage of X ray tube was 40 kV. The working electric current was 40 mA. The scanning degree 2θ is from 10° to 80° with step size 0.013° and scan step time 53.3 s.

Scanning electron microscope with energy dispersive spectroscopy (SEM–EDS)

SEM–EDS analysis was performed on HITACHI TM3030 scanning electron microscope under low vacuum mode with a working voltage of 15 kV.

Pyrolysis-gas chromatography/mass spectrometry (Py-GC–MS)

The Py-GC–MS was performed on Agilent Technologies 8860/5957C inert MSD chromatograph/mass spectrometer equipped with Frontier EGA/PY-3030D pyrolyzer. Samples were placed into a 50 μl stainless steel Eco-cup fitted with an Eco-stick, and 5 μl of 10% tetramethylammonium hydroxide (TMAH) solution were introduced for derivatization. After three minutes, the cup was placed into the pyrolysis interface where it was purged with helium for three minutes. Samples were pyrolyzed using a single-shot method at 550 °C. An Agilent 122-5532UI capillary column was used for separation (30 m × 250 μm × 0.25 μm) with helium carrier gas set to 1 ml/min. The split injector was set to 320 °C with a split ratio of 50:1 and no solvent delay. The GC oven temperature program was 40 °C for 2 min, then ramped to 320 °C at 6 °C/min, followed by a 9 min isothermal period. The MS transfer line was at 320 °C, the source at 230 °C, and the MS quad at 150 °C. The mass spectrometer was scanned from 33 to 600 amu at a rate of 2.59 scans per second. The electron multiplier was set to the autotune value. The resulting total ion chromatograms and associated mass spectra processed and interpreted using Agilent Masshunter Workstation and NIST17 database.

Thermal analysis

Thermogravimetry, derivative thermogravimetry and differential scanning calorimetry (TG-DTG-DSC) analysis was performed on synchronous thermal analyzer (Q600 SDT TA Instruments). The experimental temperature was increased from room temperature to 800 °C at a heating rate of 20 °C/min under nitrogen-gas dynamic atmosphere (100 ml/min).

Results and discussion

Identification of the putty components

After observing the apparent structures of the samples shown in Fig. 1, we first applied FTIR analysis to qualitatively determine the basic compositions of them. All the examined samples in Fig. 2 show pronounced absorptions at 1410 cm^{-1} (asymmetric stretching of CO_3^{2-}) and 872 cm^{-1} (CO_3^{2-} deformation), indicating the main matrix is calcite [17]. It was also confirmed by XRD in Fig. 3, showing the calcite is the dominant crystalline phase with impurities quartz and pyrite. In the ancient literature "Tian Gong Kai Wu", translated as "Exploitation of the works of nature", the technique of making lime from oyster shell was recorded and called as "oyster ashes", which was an important lime source of coastal areas. As the ship was constructed in Fujian, "oyster ashes" was probably one of the raw materials.

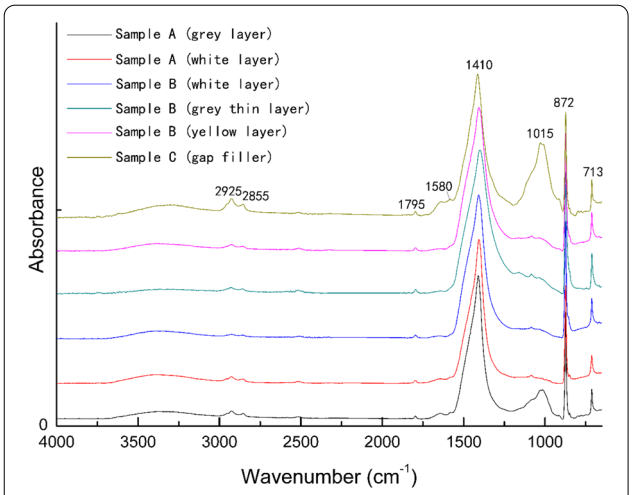

Fig. 2 FTIR spectra of the putty samples

The bands around 2925 cm^{-1} and 2855 cm^{-1} in Fig. 2 corresponding to saturated C–H stretching vibrations suggest there are minor addition of organic matters (probably oil) within these white or yellowish samples. For the grey layer, white layer of sample A, yellow layer of sample B and sample C, there are extremely weak but still noticeable absorptions at 1580 cm^{-1} in Fig. 2 corresponding to asymmetric stretching vibration of carboxylic anion. However, there is no absorption from 1750 to 1700 cm^{-1}, suggesting most of the oil has been converted to carboxylate. Except the gap sealer (sample C), all of the others show very weak absorptions from organic matters, which can hardly tell the difference regarding to the relative amount of organic matters, no matter what their color are. Only the grey layer of sample A shows a little bit stronger absorption at around 1000 cm^{-1}, which suggests either larger proportion of organic matters or better preservation of them. The gap sealer (sample C) presents the most evident absorption at 2925, 2855, and 1015 cm^{-1}, consistent with the remained cellulosic fiber after washed by 5% HCl solution, shown in Fig. 4. The fibers in Fig. 4 exhibit large and round or polygon lumens, which are consistent with jute fibers [14].

The soluble organic matters from sample C were extracted by ethyl acetate after acidification, which can form brown film at room temperature and become sticky when it is slightly heated. The FTIR spectrum of it (Fig. 5) shows strong absorption at 2926, 2855and 725 cm^{-1} corresponding to saturated C–H stretching and deformation in long aliphatic chains. Another strong absorption at 1707 cm^{-1} suggests carboxyl is the major functional group. Additionally, the absorptions at 969, 949, 938 and 3014 cm^{-1} further suggest the existence of C=C bonds [18]. The above absorptions of the extracted film FTIR spectrum confirm fatty acids as the main extractable component in the putty. The original

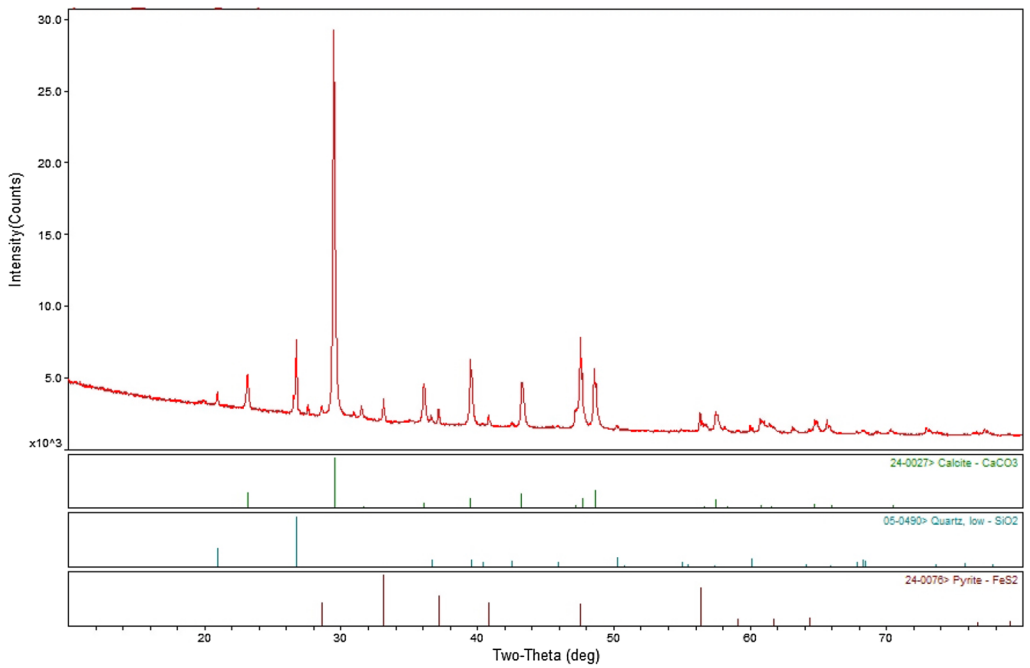

Fig. 3 XRD spectrum of sample B

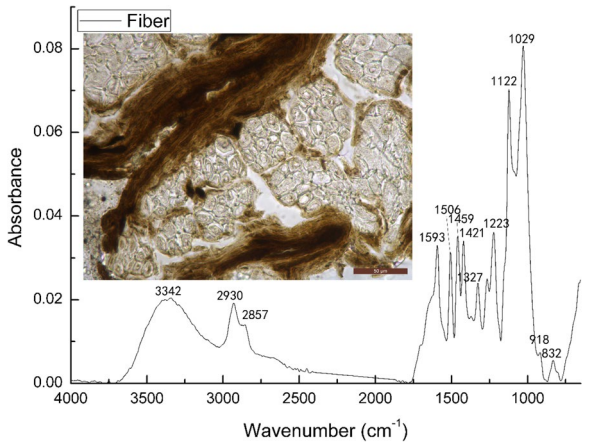

Fig. 4 FTIR spectrum and microstructure of the fibers in sample C

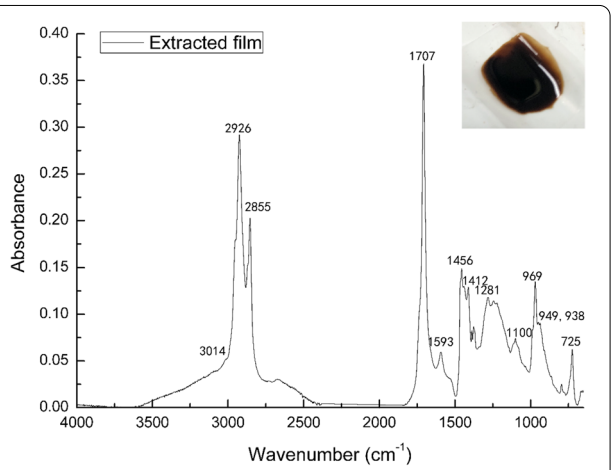

Fig. 5 FTIR of the organic extract of sample C

oil in the putty were saponified in the form of calcium carboxylate according to the absorption at 1580 cm^{-1} in Fig. 2.

Further analysis by Py-GC–MS of the organic extract of sample C was carried out to confirm the use of Tung oil. Shown in Fig. 6a, b, (9Z,11E,13E)-octadeca-9,11,13-trienoic acid (methyl ester) or eleostearic acid (methyl ester) was directly found in the sample C. Also, another special compound shown in Fig. 6a, c, 9-(*o*-propylphenyl)-nonanoic acid (methyl ester), was identified. This special compound was only found in boiled Tung oil and not found in raw Tung oil or other drying oils, which is thus proposed by Wang N as the marker for identification of Tung oil though py-GC–MS technique [19]. As it was only found in boiled Tung oil but not found in raw Tung oil, it is reasonable to infer that the formation of it might involve the rotation of the second double bond of conjugated triene [20] from eleostearic acid followed by thermal 6π-electrocyclization [20, 21] during the boiling process of Tung oil and aromatization of 1,3-cyclohexadiene moiety by dehydrogenation. Additionally, the ratio of palmitic acid and stearic acid (P/S) is 1.41, consistent with the reported value of Tung oil [19, 22].

The microscopic layered structures of the samples

SEM–EDS analysis was applied to further observe the layered structures of the surface coating samples. Each spot marked in number in Fig. 7 corresponds to the same entry number in Table 1. The cross-section of the black and white layers of sample A is shown in Fig. 7a, b. There are more than two layers in the black and white layer complex. By comparing Fig. 7a, b, the white layer can be further divided into one white sub-layer with thickness of 233–392 μm and one pale yellow sub-layer with thickness of 94–201 μm. EDS results show that the white layer has a Ca/C/O ratio of 1:1.2:3.4 (shown in Table 1 entry 1), which matches calcite with minor organics. However, the pale yellow layer has a Ca/C/O ratio of 1:4.5:4.6 (shown in Table 1 entry 2), which suggests high content of Tung oil. Considering the pale yellow layer is very thin and uniform, it could be formed by either brushing with Tung oil or with putty high in Tung oil content. Because the grey layer of sample A is very loose and easy to detach, it was observed separately and shown in Fig. 7c. The grey layer of sample A shown in Fig. 7c is uniform with a thickness of 600–814 μm and has a close composition to calcite shown in Table 1 entry 4.

The outer black layer of sample A is mixed with crystals and rod-shape particles. The black layer of sample A seemed to be very unusual as it was never seen on any other lime putties reported in previous researches. The brighter crystals in Fig. 7a, d are featured with regular octahedron and its combinate framboids, which indicating they belong to cubic system. The Fe/S ratio of these crystals is 1:1.16 shown in Table 1 entry 5, suggesting they are pyrite or other sulfur-iron compounds' pseudomorph after pyrite. The porous rods with delicate structure in Fig. 7e have a close composition to calcite (shown in Table 1 entry 3 and 6) and was likely to formed through deposition of calcite on their original framework from ocean creatures. Therefore, the color of the black layer is caused by sulfur-iron compounds such as pyrite and the whole black layer was not original but formed during the burial in the seabed.

The white layer of sample B shown in Fig. 1f is about 2.6 mm thick and the yellow layer is about 2.4 mm in thickness. In the middle of the two layers, there is an intermediate thin grey layer, which looks more compact in Fig. 7f with a thickness of 194–785 μm. The Ca/C/O ratios of the white layer (shown in Table 1 entry 7) and the grey thin layer (shown in Table 1 entry 8) are both

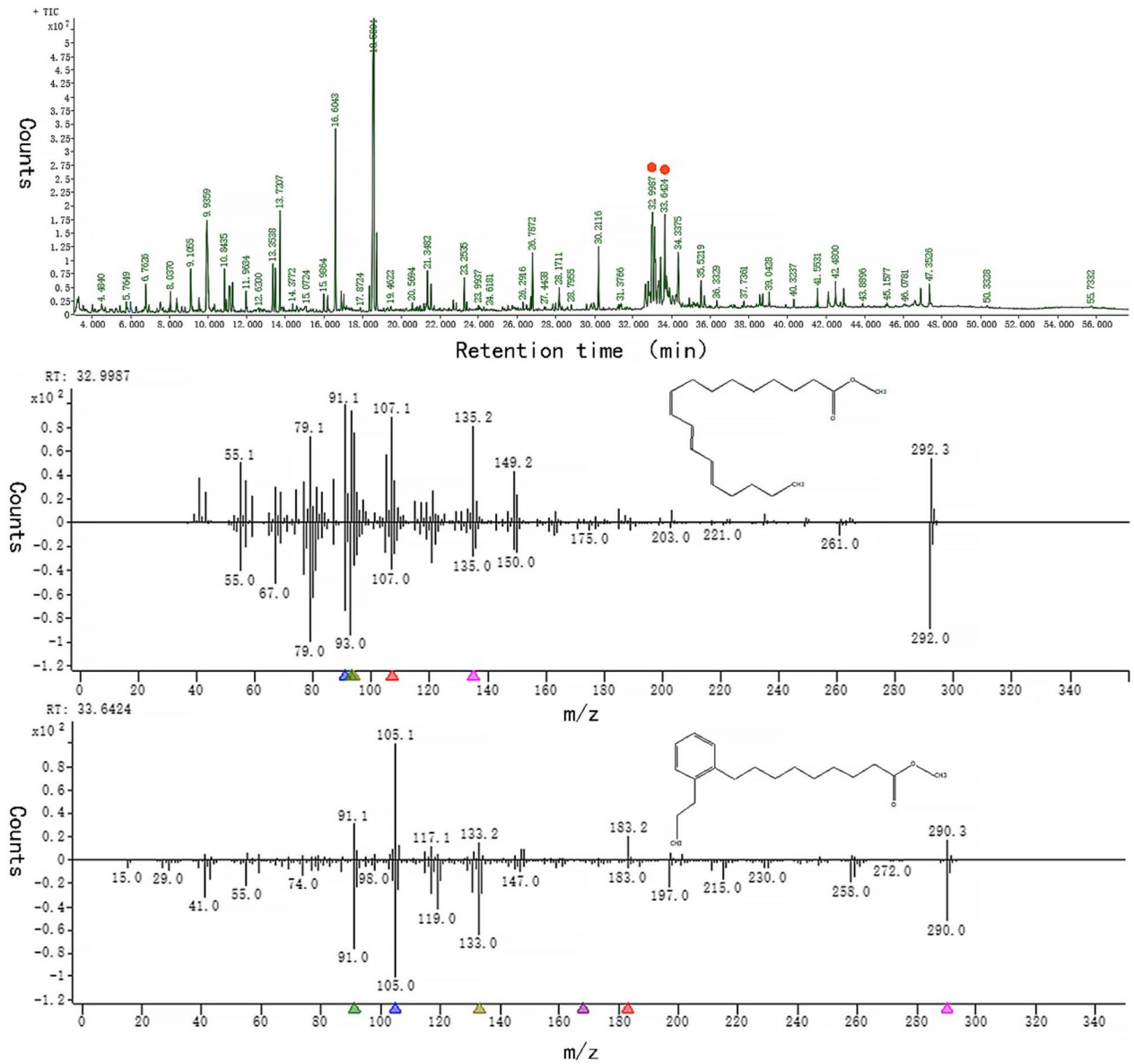

Fig. 6 TIC and selected MS spectra of sample C

1:1:2.8 and matches calcite, while the carbon content in the yellow layer is slightly higher (shown in Table 1 entry 9) and Ca/C/O ratio is 1:2.1:4.2, which indicates it contains more Tung oil.

In both sample A and sample B, there are outer yellow or pale yellow layers and inner white layers. For sample A, there is an additional innermost grey layer. In both samples, it is hard to separate the yellow layer and the white layer from each other whereas the grey layer of sample A are very easy to detach. One possible explanation is that during the use of the ship, the coating materials should be regularly renewed before they became ineffective and therefore new layers were applied. If assuming the yellow layer and the white layer were successively applied as a normal coating process, then there should be another yellow layer between the white layer and the grey layer of sample A. In this case, the previous layer might be removed before new putties were applied and the old layer of sample A were not completely removed somehow, which seems to be farfetched. If assuming each layer representing one renewal coating process, then the difference in Tung oil content is hard to explain and the interface between the layers shouldn't be such smooth and clean. Instead,

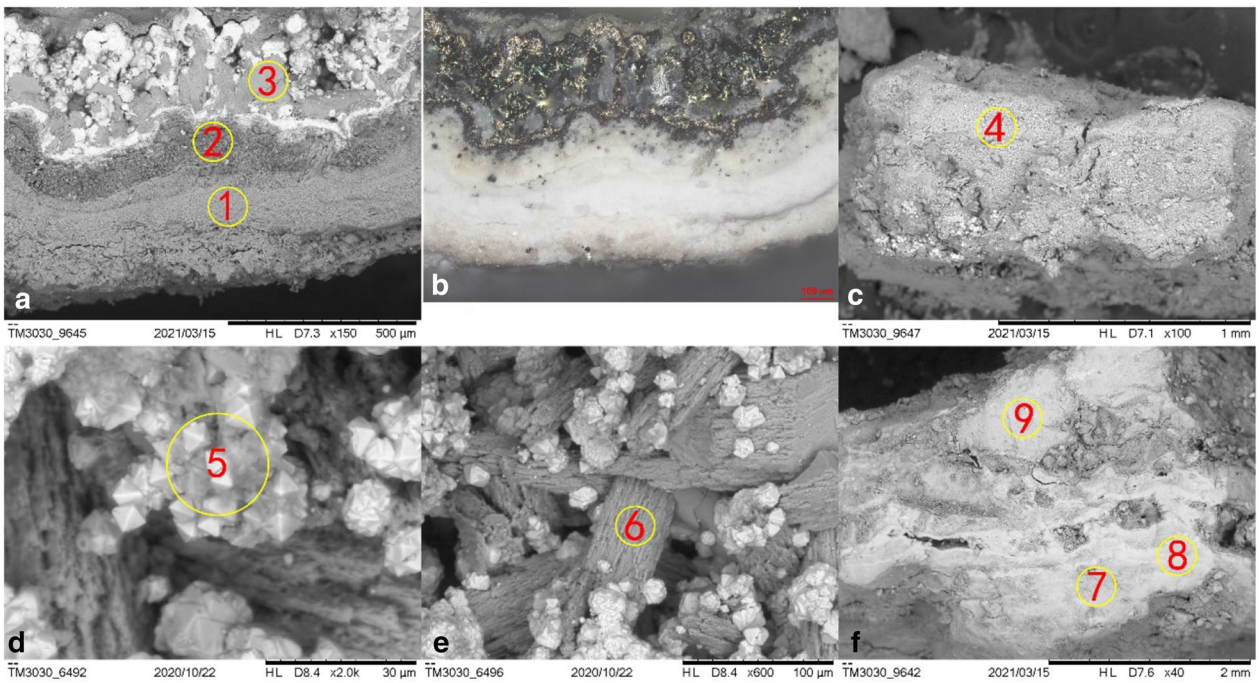

Fig. 7 Micrographs of **a** cross-section of sample A's black and white layers under SEM, **b** cross-section of sample A's black and white layers under optical microscope, **c** cross-section of sample A's grey layer, **d** pyrite crystals on the surface of sample A, **e** rod-shape calcite on the surface of sample A, and **f** cross-section of sample B layers under SEM

Table 1 Elemental compositions of the corresponding spots in Fig. 7 shown in at.%

Spot in Fig. 7	C	O	Na	Mg	Al	Si	S	Cl	K	Ca	Fe
1	21.44	59.18	0.03	1.16	–	0.12	0.25	–	0.20	17.51	0.11
2	43.49	44.42	0.11	0.51	0.08	0.04	1.12	0.07	0.05	9.61	0.51
3	20.47	55.68	0.26	0.41	0.22	0.52	0.93	0.05	0.22	20.63	0.62
4	26.63	56.60	0.20	0.67	0.11	0.22	0.13	–	–	15.33	0.11
5	28.02	22.04	–	0.78	2.76	4.31	21.41	–	0.10	2.19	18.40
6	26.66	46.44	–	–	–	0.46	2.78	–	–	20.74	2.91
7	20.58	56.79	0.44	0.33	0.04	0.33	0.46	0.23	–	20.36	0.44
8	20.54	57.69	0.24	0.11	–	–	0.69	0.12	–	20.60	–
9	27.42	55.48	0.73	0.90	0.42	0.93	0.73	0.04	–	13.35	0.01

sediments should present between each layer. It is more likely that the layer attached to the wood plank was influenced by organic acids produced by wood deterioration. The decomposition of part of calcite by organic acids could cause the inner part of the white layer becoming loose and dark colored organic molecules released from wood could cause the grey color. In the meantime, it might be more economical to apply an inner putty layer with lower Tung oil content and cover it with a putty layer with a higher Tung oil content to ensure the required performances.

Quantitative study by thermal analysis

It would be more desirable if the relative amounts of organic and inorganic components are determined. Therefore, TG analysis was applied. As shown in Fig. 8, the TG–DTG–DSC curves can be divided into five parts, i.e., approximately 20–150 °C, 150–400 °C, 400–500 °C, 500–600 °C and 600–800 °C. The first range is assigned to water losses and the second range is assigned to decomposition of ordinary organics. However, calcium carboxylate has better thermostability than other organics. The third range exhibits evident DTG peaks at around 457 °C,

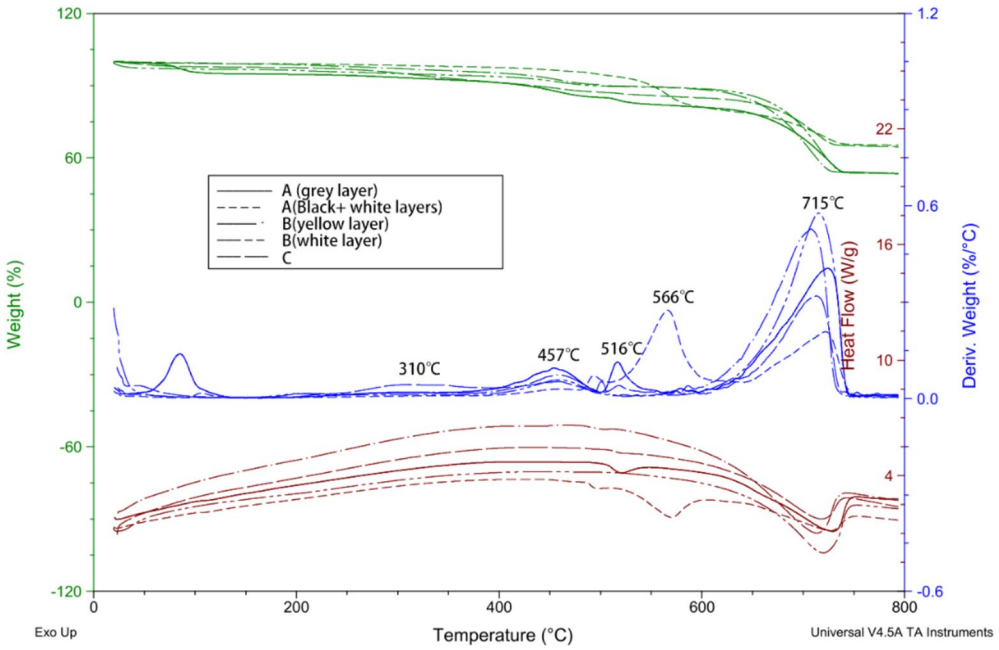

Fig. 8 TG-DTG-DSC of the putty samples

which are assigned to the calcium carboxylate of Tung oil with reference to thermal analysis of calcium carboxylate prepared from Tung oil (shown in Additional file 1). The DTG peak at around 457 °C was also noticed in previous analysis on the sample from Baochuanchang [15], but possibly mistaken as inorganic impurities. The fourth range might involve various mineral impurities from sediments. For sample A (white + black layer), there is an considerable weight loss and endothermic peak at around 566 °C, which matches the decomposition of pyrite, producing elemental sulfur [23]. The fifth range is the decomposition of calcite. Tung oil exhibits exothermic peak and weight loss at around 320 °C [16] during thermal analysis. But the weight losses of all the samples from 150 to 400 °C were extremely low, suggesting very poor preservation of the organic matters except the calcium carboxylate. The weight loss of the calcium carboxylate involved decomposition of aliphatic moieties and formation of calcite and should be converted to the weight of Tung oil when estimating the ratio of lime ($Ca(OH)_2$) and Tung oil. In the meanwhile, the weight loss of CO_2 in the fifth range included the decomposition of calcite formed during the decomposition of the calcium carboxylate. Also, the weight losses from 150 to 400 °C should be added, though these organics are probably deteriorated and impossible to deduce the original weight. Based on the TG data, the calculated ratios of $Ca(OH)_2$/organics are shown in Table 2. The ratios of all the samples range from 3.1:1 to 7.9:1. Since sample C contains jute fibers, the true ratio of $Ca(OH)_2$/Tung oil is higher than the calculated $Ca(OH)_2$/organics ratio. Except sample C, the ratios of $Ca(OH)_2$/organics of sample A's grey

Table 2 Quantitative TG results of the putty samples

	Weight loss (150–400 °C)	Weight loss (400–500 °C)[a]	Weight loss (600–800 °C)	Calculated ratio of $Ca(OH)_2$/organics
Sample A (grey layer)	3.7%	6.1%	27.6%	4.3
Sample A (white + black layer)	1.6%	1.8%	15.7%	7.1
Sample B (yellow layer)	3.8%	4.8%	34.8%	6.2
Sample B (white layer)	3.0%	3.8%	35.2%	7.9
Sample C	6.4%	4.0%	20.4%	3.1

[a] The range for sample A (white + black layer) is 400–478 °C and that for sample B (yellow layer) is 400–496 °C due to evident weight losses of impurities at around 490–500 °C

layer as 4.3:1 are the highest. As previously mentioned, the grey layer could be formed under the impact of wood deterioration. The decomposition of calcite by organics acids from wood would reduce the relative content of calcite, causing the $Ca(OH)_2$/organics ratio lower than its true value. Though the yellowish sub-layer of sample A was unable to be analyzed alone, the ratio of $Ca(OH)_2$/organics of it should be lower than that of the black and white layers as 7.1:1. Also, the ratio of the yellow layer of sample B (6.2:1) are higher than the white layer of sample B (7.9:1). The outer layer is normally presumed to be more prone to deteriorated. However, both yellow outer layers of samples A and B display lower ratios than those of the corresponding white layer, which suggests deterioration can hardly explain the difference in the $Ca(OH)_2$/organics ratios. For sample C, it is impossible to exclude the contribution of the jute fiber to the weight loss accurately. The $Ca(OH)_2$/organics ratio of sample C as 3.1:1 indicates the ratio of $Ca(OH)_2$/Tung oil would be higher than 3.1:1. If only considering the weight loss of calcium carboxylate and omitting other organics, then the ratio of $Ca(OH)_2$/Tung oil should be no more than 7.3:1.

Previous studies suggest the ratio of $Ca(OH)_2$/Tung oil for ship use are 1.4:1 [16] and 3:1 [24]. According to historical records of the Ming Dynasty, the ratio was 2:1 or 3:1 for most river boats and warships [25, 26]. The ratio of $Ca(OH)_2$/Tung oil of Nanhai I samples are obviously higher than the sample from Baochuanchang shipyard and records from historical documents. It must be considered that the ships built in Baochuanchang shipyard were royal warships, which must be constructed by the highest standard. Therefore, it is not surprised that the $Ca(OH)_2$/Tung oil ratio of the Baochuanchang sample is as low as 1.4:1. On the contrary, Nanhai I was a merchant ship and high cost-effectiveness should be its typical feature. Although higher Tung oil content can provide better mechanical and waterproofing performances, it is not necessarily more economical. It can be an economical way by overall reducing Tung oil content in the putties and raising Tung oil content in the outer layer to meet the performance requirements.

Conclusion

In this paper, the sealing materials of the merchant ship Nanhai I of the Southern Song Dynasty were analyzed via several analytical techniques to characterize it components and structures. Overall, the sealing materials are confirmed by FTIR, XRD and Py-GC/MS as typical Chinese Chu-nam putty, an inorganic/organic mixture of lime and Tung oil. Two types of putty are found, i.e., gap filler with jute fibers and surface coating without any oakum.

There are evident layered structures in both surface coating type samples. For sample A representing thin layer putty, the outmost black layer was formed by pyrite and calcite later deposited, which can be ignored when discussing its original layered structure. Except the outmost black layer, sample A can be divided into an outer white layer and an inner grey layer by naked eyes and the white layer can be further divided into an outer thin yellowish sub-layer and an inner white sub-layer under microscope. EDS results show that the outer thin yellowish layer contains considerably high content of carbon, which suggests a layer with higher Tung oil content or an additional coating of Tung oil. Sample B representing thicker layer putty can be divided into an outer yellow layer and an inner white layer. The yellow layer shows higher carbon content than the white layer. Quantitative analysis by thermal analysis suggests the ratio of $Ca(OH)_2$/Tung oil range from 4.3:1 to 7.9:1 for surface coating type samples A and B, and the ratio of $Ca(OH)_2$/organics is 3.1:1 for the gap filler sample C. The $Ca(OH)_2$/Tung oil ratio of the innermost grey layer of sample A (4.3:1) are the lowest. However, it is likely that the grey loose layer was eroded by organic acids released from wood deterioration, causing the low ratio and it could be originally the white layer. The yellow layer of sample B shows lower ratio of $Ca(OH)_2$/Tung oil (6.2:1) than that of the white layer of sample B (7.9:1). It is inferred that the composite layers with different Tung oil contents could be a result of balancing the costs and performances of the putty.

So far, there is not adequate reports on the sealing materials of ancient Chinese ships to fully understand the technical aspects of them. This paper may help study the application of lime putties on ancient Chinese ships and provide important reference to the restoration or conservation of shipwrecks such as Nanhai I.

Supplementary Information

The online version contains supplementary material available at https://doi.org/10.1186/s40494-021-00523-2.

Additional file 1. Thermal analysis of the calcium carboxylate prepared from Tung oil.

Acknowledgements

We sincerely thank Qin Yang and Li Ding from the National Museum of China for assisting the analysis of Py-GC/MS.

Authors' contributions

All the experiments were designed and carried out by YZ. The data were analyzed by YZ and KW. The sample was collected with the help of JS and YC. The manuscript was written by YZ and revised by KW and DH. All authors read and approved the final manuscript.

Funding
The research is supported by National Social Science Foundation of China (Grant No. 19CKG032).

Availability of data and materials
The datasets analyzed during the current study are available from the corresponding author on reasonable request.

Declarations

Competing interests
There is no financial and non-financial competing interests.

Author details
[1]School of Archaeology and Museology, Peking University, Beijing, China. [2]Underwater Cultural Heritage Protection Centre, State Administration of Cultural Heritages, Beijing, China. [3]Guangdong Provincial Institute of Cultural Relics and Archaeology, Guangdong, China.

Received: 26 January 2021 Accepted: 21 April 2021
Published online: 30 April 2021

References

1. National Center of Underwater Cultural Heritage, Guangdong Institute of Cultural Relics and Archaeology, Chinese Academy of Cultural Heritage, et al. The excavation report of Nanhai I shipwreck, vol. 2. Beijing: Cultural Relics Press; 2018. **(in Chinese)**.
2. Lin T. Discussion of iron wares carried by Nanhai No. 1. Study Nat Cult Herit. 2018;8:66–71 **(in Chinese)**.
3. Li Y. Brief study on gold leaves unearthed from Nanhai I shipwreck. Museum. 2020;23:10–4 **(in Chinese)**.
4. Rani SD, Rahul AV, Santhanam M. A multi-analytical approach for pore structure assessment in historic lime mortars. Constr Build Mater. 2020;272:121905.
5. Ali MF, Moussa A, Abdelhafez M. Alternative lime based grouts used in re-pointing of deteriorated ancient mortars and their structural effects on composite unreinforced masonry walls of Mekaad Radwan, Ottoman Cairo, Egypt (case study). Procedia Soc Behav Sci. 2016;225:410–20.
6. Santhanam K, Shanmugavel D, Ramadoss R, Arakatavemula V. Characterisation on ancient mortar of Chettinadu house at Kanadukathan, Karaikudi, Tamil Nadu, India. Mater Today Proc. 2020. https://doi.org/10.1016/j.matpr.2020.08.607.
7. Azeiteiro LC, Velosa A, Paiva H, Mantas PQ, Ferreir VM, Veiga R. Development of grouts for consolidation of old renders. Constr Build Mater. 2014;50:362–360.
8. Iucolano F, Liguori B, Colella C. Fibre-reinforced lime-based mortars: a possible resource for ancient masonry restoration. Constr Build Mater. 2013;38:785–9.
9. Fang S, Zhang Q, Zhang H, Zhang B. A study of traditional blood lime mortar for restoration of ancient buildings. Cem Concr Res. 2015;76:232–41.
10. Zhang K, Sui Y, Wang L, Tie F, Zhang Y. Effects of sticky rice addition on the properties of lime-tile dust mortars. Herit Sci. 2021;9:4.
11. Wang S, Wang S, Lu Z, Yao W, Liu B, Li B. Characterization of sticky-rice lime binders from old masonry relics in north china: the primary contribution for conservation. Constr Build Mater. 2020;250:118887.
12. Nemecek J, Nezerka V, Slizkova Z, et al. Investigation of crushed brick-matrix interface in lime-based ancient mortar by microscopy and nanoindentation. Cem Concr Compos. 2015;55:122–8.
13. SarpTunçoku S, Caner-Saltık EN. Opal-a rich additives used in ancient lime mortars. Cem Concr Res. 2006;36:1886–93.
14. Fang S, Zhang H, Zhang B, Wei G, Li G, Zhou Y. A study of the Chinese organic-inorganic hybrid sealing material used in "Huaguang No.1" ancient wooden ship. Thermochim Acta. 2013;551:20–6.
15. Gong Y, Li C, Yu X, Wang J, Gong D. Study on the ancient putty from the site of the Ming Dynasty (1368–1644 CE) Baochuanchang shipyard, Nanjing, China. J Archaeol Sci Rep. 2019;23:189–95.
16. Yu X, Li C, Wang J, Gong D. Quantitative study on the sealing material of 600 years ago. Thermochim Acta. 2017;653:79–82.
17. Reig FB, Adelantado JVG, Moreno MCMM. FTIR quantitative analysis of calcium carbonate (calcite) and silica (quartz) mixtures using the constant ratio method. Appl Geol Samples Talanta. 2002;58:811–21.
18. Chisholm MJ, Hopkins CY. Conjugated fatty acids of Tragopogon an Calendula seed oils. Can J Chem. 1960;38:2500–7.
19. Wang N, He L, Zhao X, Simon S. Comparative analysis of eastern and western drying-oil binding media used in polychromic artworks by pyrolysis-gas chromatography/mass spectrometry under the influence of pigments. Microchem J. 2015;123:201–10.
20. Wei S, Li Y, Ma Q, Lou S, Schreiner M. Characterization of Tang Dynasty lamp oil remains by using pyrolysis gas chromatography and mass spectrometry. J Analyt Appl Pyrol. 2015;116:237–42.
21. Doering WVE, Roth WR, Bauer F, et al. Rotationsbarrieren vinyl-substituierter olefine. Chem Ber. 1991;124:1461–70.
22. Diedrich MK, Hochstrate D, Klärner FG, et al. The pressure effect in pericyclic rearrangements: the cope rearrangement, electrocyclization, and the intramolecular Diels–Alder reaction. Angew Chem Int Ed. 1994;33:1079–81.
23. Labus M. Pyrite thermal decomposition in source rocks. Fuel. 2021;287:119529.
24. Fang S, Zhang H, Zhang B, Li G. A study of Tung-oil-lime putty—a traditional lime based mortar. Int J Adhes Adhes. 2014;48:224–30.
25. Shen Q, Ren J. Records of the Southern Ships (Nan Chuan Ji). Henan: Henan Education Publishing House; 1994. p. 427–66 **(in Chinese)**.
26. Li Z. Records of the Longjiang Shipyard (Long Jiang Chuan Chang Zhi). Nanjing: Jiangsu Classic Publishing House; 1999. p. 189–252 **(in Chinese)**.

Publisher's Note